Journal of Medicinal Chemistry Article

J. Med. Chem. **2010,** *53,* 6923–6933 **6923**
DOI: 10.1021/jm1004804

Development of Bimetallic Titanocene−Ruthenium−Arene Complexes As Anticancer Agents: Relationships between Structural and Biological Properties

Frédéric Pelletier,[†] Virginie Comte,[†] Alexandre Massard,[†] Margot Wenzel,[†] Stéphanie Toulot,[†] Philippe Richard,[†] Michel Picquet,*[,†] Pierre Le Gendre,[†] Olivier Zava,[‡] Fabio Edafe,[‡] Angela Casini,*[,‡] and Paul J. Dyson[‡]

[†]*Institut de Chimie Moléculaire de l'Université de Bourgogne, UMR 5260 CNRS—Université de Bourgogne, 9 Avenue A. Savary, BP 47870, 21078 Dijon, France, and* [‡]*Institut des Sciences et Ingénierie Chimiques, Ecole Polytechnique Fédérale de Lausanne (EPFL), CH-1015 Lausanne, Switzerland*

Received April 19, 2010

A series of bimetallic titanium−ruthenium complexes of general formula $[(\eta^5\text{-}C_5H_5)(\mu\text{-}\eta^5{:}\kappa^1\text{-}C_5H_4\text{-}(CR_2)_nPR'R'')TiCl_2](\eta^6\text{-}p\text{-cymene})RuCl_2$ (n = 0, 1, 2 or 4; R = H or Me; R′ = H, Ph, or Cy; R″ = Ph or Cy) have been synthesized, including two novel compounds as well as two cationic derivatives of formula $[(\eta^5\text{-}C_5H_5)(\mu\text{-}\eta^5{:}\kappa^1\text{-}C_5H_4(CH_2)_nPPh_2)TiCl_2]$ $[(\eta^6\text{-}p\text{-cymene})RuCl](BF_4)$ (n = 0 or 2). The solid state structure of two of these compounds was also established by X-ray crystallography. The complexes showed a cytotoxic effect on human ovarian cancer cells and were markedly more active than their Ti or Ru monometallic analogues titanocene dichloride and RAPTA-C, respectively. Studies of cathepsin B inhibition, an enzyme involved in cancer progression, showed that enzyme inhibition by the bimetallic complexes is influenced by the length of the alkyl chain in between the metal centers. Complementary ESI-MS studies provided evidence for binding of a Ru(II) fragment to proteins.

Introduction

The pioneering discovery of the anticancer activity of cisplatin by Rosenberg in 1969[1] opened the way to metal-based drugs in the fight against cancer. Indeed, platinum-based drugs are nowadays among the most effective clinical agents for the treatment of cancer, with cisplatin, carboplatin, and oxaliplatin being the most widely used.[2] However, their effectiveness is still hindered by clinical problems, including acquired or intrinsic resistance that limits the spectrum of cancers that can be treated, and high toxicity leading to side effects and limiting the dose that can be administrated.[3] Consequently, efforts have focused on the development of other platinum-based drugs[4] as well as metallodrugs based on other metal centers.[5] Among the thousands of inorganic derivatives synthesized and tested, only three nonplatinum-based complexes have reached phase II clinical trials, namely the organometallic compound titanocene dichloride ($Ti(\eta^5\text{-}C_5H_5)_2Cl_2$)[6] and the Ru-based coordination compounds KP1019[7] and NAMI-A[8] (Figure 1).

Because of the promise of these metallodrugs, increasing interest has thus turned to the development of ruthenium- and titanium-based anticancer compounds, among others. Of particular interest, investigations into the anticancer activity of organometallic Ru(II)−arene derivatives is gaining increasing attention.[9] Ru−arene complexes containing a phosphine ligand, such as $[Ru(\eta^6\text{-}C_6H_6)(pta)Cl_2]$ (RAPTA-B) and $[Ru(\eta^6\text{-}p\text{-}C_{10}H_{14})(pta)Cl_2]$ (RAPTA-C) (pta = 1,3,5-triaza-7-phosphaadamantane) (Figure 1) show very promising in vivo activities on the inhibition of metastasis growth,[10] together with a high selectivity and low general toxicity.[11]

In parallel, following the failure of titanocene dichloride to fulfill the criteria required in phase II clinical trials, modification of its Cp-ligands via the introduction of various functional groups, such as amines[12] and ether[13] moieties, led to a revival in the field.[14] The different physico- and biochemical properties of these new Ti(IV) complexes (viz. solubility in aqueous media, hydrolytic stability, and hydrogen bonding toward DNA) resulted in superior antitumor activity in some cases (Figure 1).[15]

For all the above-mentioned Ru- and Ti-based metal complexes, their mechanism of pharmacological action remains poorly understood.[16] Several studies suggest that RAPTA compounds work on molecular targets other than DNA, implying a biochemical mode of action profoundly different from classical platinum anticancer drugs. Indeed, it is likely that the mechanism of action of the RAPTA complexes may involve interactions with critical intracellular or even extracellular proteins.[9h,17] Within this frame, we have recently reported on the in vitro inhibitory properties of ruthenium complexes, including RAPTA compounds, against cathepsin B (EC 3.4.22.1, cat B[a]),[18] a lysosomal papain-family cysteine protease involved in cellular metabolism processes and implicated in tumor progression and metastasis,[19] processes that RAPTA compounds have been shown to inhibit.[10a,20] In addition, modeling studies on the cat B active site were able to provide probable structures of selected RAPTA−protein adducts showing direct coordination of the Ru-center to the active site cysteine.[18a] Depending on their localization, cathepsins can be involved in two apparently opposing mechanisms of cancer progression, i.e. tumor invasion and apoptosis.[19]

*To whom correspondence should be addressed. For M.P.: E-mail: michel.picquet@u-bourgogne.fr. Tel: +33 3 80393773. Fax: +33 3 80396098. For A.C.: E-mail: angela.casini@epfl.ch. Tel: +41 21 6939860. Fax: +41 21 6939885.

[a] Abbreviations: cat B, cathepsin B; ESI-MS, electrospray ionization mass spectrometry; hCAII, human carbonic anhydrase II; Ub, ubiquitin.

Published on Web 09/07/2010

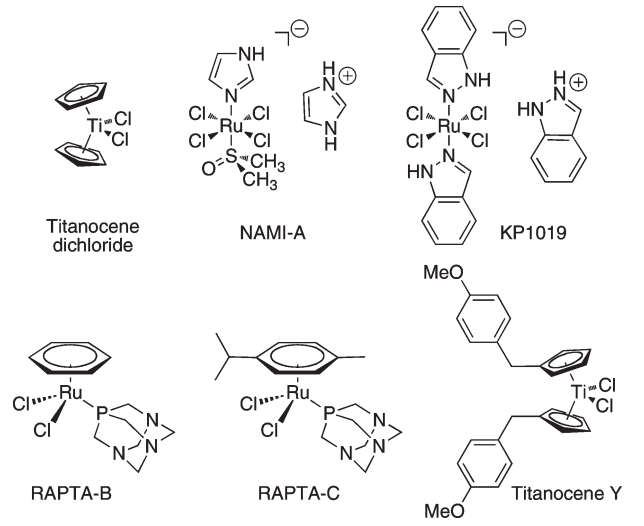

Figure 1. Nonplatinum-based metallodrugs.

Scheme 1. Synthesis of the Ruthenium−Titanocene Bimetallic Complexes **7**−**12**

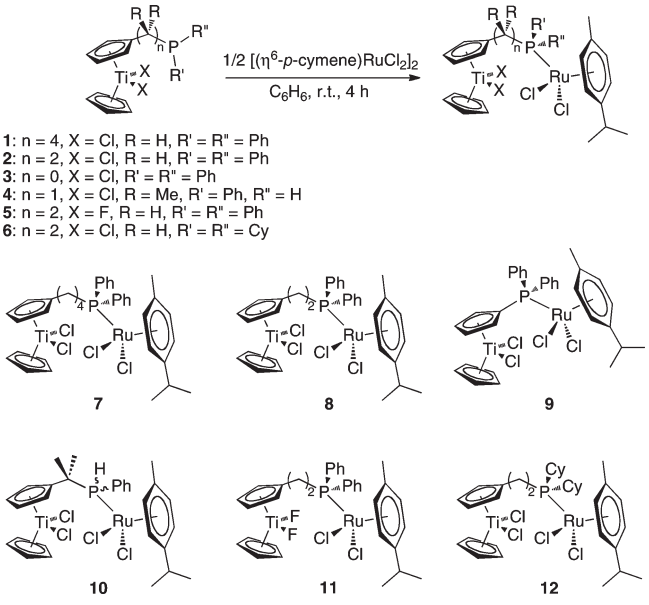

Cysteine cathepsins that are secreted or are associated with the plasma membrane participate in tumor invasion through proteolitic cascade activation, extracellular matrix degradation, and inactivation of cell-adhesion proteins, whereas intracellular proteolysis by cathepsins can trigger apoptosis.

In the case of Ti(η^5-C_5H_5)$_2$Cl$_2$, it has been postulated that binding to DNA plays a major role in the therapeutic action of the compound[21] although interactions with proteins might also be involved.[22]

A number of bi- and polymetallic complexes, either homo-[23] or heterometallic,[9m,24] have been evaluated as anticancer agents. On the ground of these previous studies, and considering that *multinuclearity* may lead to innovative chemical and biological properties,[9m] we have developed a series of heteronuclear Ti−Ru complexes based on a titanocene−phosphine backbone.[25] As far as we are aware, bimetallic Ti−Ru complexes have not been previously investigated, and our aim was to elucidate cooperative effects of these two metals when associated in the same molecule, either in terms of interacting with multiple biological targets or in terms of compound stability and favorable physicochemical properties.

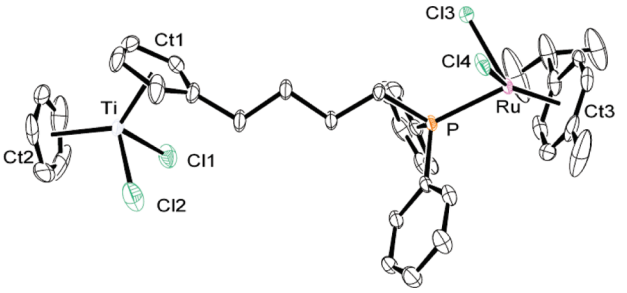

Figure 2. ORTEP view of [(η^6-*p*-cymene)[(η^5-C_5H_5)(μ-η^5:κ^1-C_5H_4-$(CH_2)_4PPh_2$)TiCl$_2$]RuCl$_2$] (**7**). Thermal ellipsoids are drawn at the 30% probability level, and solvate molecules have been omitted for clarity. Selected bond lengths (Å) and angles (deg): Ti−Ct1, 2.057(4); Ti−Ct2, 2.058(3); Ti−Cl1, 2.338(2); Ti−Cl2, 2.365(2); Ru−Ct3, 1.703(3); Ru−Cl3, 2.4104(17); Ru−Cl4, 2.4198(14); Ru−P, 2.3457(13); Ct1−Ti−Ct2, 132.1(2); Cl1−Ti−Cl2, 92.33(10); Ct3−Ru−P, 130.51(11); Ct3−Ru−Cl3, 126.43(13); Ct3−Ru−Cl4, 126.47(13); P−Ru−Cl3, 85.25(5); P−Ru−Cl4, 87.02(5); Cl3−Ru−Cl4, 86.73(7).

Results and Discussion

The novel titanocene−phosphine **1** was obtained from the reaction of lithium diphenylphosphide on (4-bromobutyl)-cyclopentadiene followed by condensation with the corresponding cyclopentadienide on CpTiCl$_3$. The secondary phosphine complex **4** was prepared using a method involving, in the initial step, the reaction of the corresponding lithium phosphide with 6,6-dimethylfulvene.[26] It is noteworthy that the ^{31}P NMR chemical shifts of −15.2 and +17.4 ppm ($^1J_{PH}$ = 206 Hz) of these two phosphines are consistent with tertiary alkyldiaryl- and secondary alkylaryl-phosphine ligands, respectively, that are not coordinated to a metal center. The corresponding bimetallic ruthenium−titanocene complexes (η^6-*p*-cymene)[(η^5-C_5H_5)(μ-η^5:κ^1-$C_5H_4(CH_2)_4PPh_2$)TiCl$_2$]RuCl$_2$ (**7**) and (η^6-*p*-cymene)[(η^5-C_5H_5)(μ-η^5:κ^1-$C_5H_4(CMe_2)PHPh$)-TiCl$_2$]RuCl$_2$ (**10**) were synthesized from the titanocene−phophines and [(*p*-cymene)RuCl$_2$]$_2$ using a literature procedure (Scheme 1).[25] According to this procedure, a slight excess of the desired phosphine is stirred in benzene for 4 h at room temperature in the presence of the ruthenium precursor. Spontaneous precipitation of the bimetallic species upon formation allows their isolation in high yield.

The ^{31}P NMR spectra of **7** and **10** contain singlets at 23.6 and at 59.8 ppm, corresponding to a downfield shift of about 40 ppm relatively to free ligands,[25] indicative of coordination of the phosphorus center to the ruthenium center. It is also worth mentioning that in the ^{1}H and ^{31}P NMR spectra of **10**, a substantial increase of the $^1J_{PH}$ coupling constant, from 208 Hz in the free titanocene−phosphine **4** to 380 Hz in the κ^1-P-coordinated derivative **10**, was observed. The structure of **7** was established in the solid state by X-ray crystallography, confirming the formation of the bimetallic complex (Figure 2).

The molecular structure of **7** is similar to that of **8** reported previously.[25] The geometry of the Cp(C_5H_4R)TiCl$_2$ fragment is as expected with the alkyl-chain lying in the open side of the bent metallocene. The arene ruthenium moiety adopts a classical three-leg piano stool conformation and exhibits the standard geometrical parameters found for 65 (η^6-*p*-cymene)-Ru(PR$_3$)Cl$_2$ fragments found in the CCDC database. The observed intramolecular intermetallic distance is 10.8137(11)

Scheme 2. Synthesis of the Cationic Ruthenium−Titanocene Bimetallic Complexes **13** and **14**

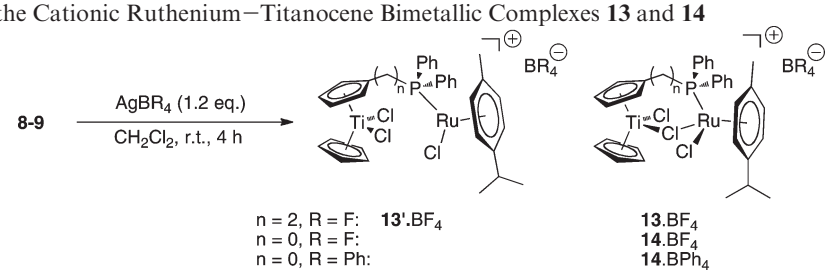

Å. (CCDC 766062 (compound **7**) and 766061 (compound **14**·BPh_4) contain the supplementary crystallographic data for this paper, which can be obtained free of charge from the Cambridge Crystallographic Data Center via www.ccdc.cam.ac.uk/data_request/cif.)

To modify the solubility of the titanocene complexes in aqueous media, the cationic derivatives **13** and **14** were prepared by chloride abstraction from the ruthenium center in the corresponding neutral compounds. Thus, (η^6-*p*-cymene)-[(η^5-C_5H_5)(μ-η^5:κ^1-$C_5H_4(CH_2)_2PPh_2$)$TiCl_2$]$RuCl_2$ (**8**) and (η^6-*p*-cymene)[(η^5-C_5H_5)(μ-η^5:κ^1-$C_5H_4PPh_2$)$TiCl_2$]$RuCl_2$ (**9**) were treated with an excess of silver tetrafluoroborate in dichloromethane at room temperature (Scheme 2).

The ^{31}P NMR spectrum of **13** contains two signals at 23.2 and 23.3 ppm in 55:45 ratio. The existence of two different species was also noted in the ^{1}H NMR spectra in which two sets of signals were observed for the two *iso*-propyl-methyl groups at 0.86, 0.94, and 0.90, 0.93 ppm or for the unsubstituted Cp ligand at 6.49 and 6.52 ppm (see Experimental Section). Moreover, the typical shape of the signals of the substituted Cp-ligand and of the aromatic protons of the arene in the minor compound, with all protons being anisochrones, reveal a rigid structure with loss of symmetry. These observations indicate the presence of the two isomers [(η^6-*p*-cymene)[(η^5-C_5H_5)(μ-η^5:κ^1-$C_5H_4(CH_2)_2PPh_2$)TiCl(μ-Cl)]RuCl]-(BF_4) (**13**·BF_4), corresponding to an 18-electron species, and [(η^6-*p*-cymene)[(η^5-C_5H_5)($\mu-\eta^5$:κ^1-$C_5H_4(CH_2)_2PPh_2$)$TiCl_2$]-RuCl](BF_4) (**13′**·BF_4), which is formally electronically unsaturated, although a weakly coordinating solvent ligand could stabilize the structure. In the case of **14**·BF_4, obtained from the corresponding neutral derivative (η^6-*p*-cymene)[(η^5-C_5H_5)(μ-η^5:κ^1-$C_5H_4PPh_2$)$TiCl_2$]$RuCl_2$ (**9**), only one resonance signal was observed at 33.3 ppm in the ^{31}P NMR spectrum. The ^{1}H NMR spectrum of **14**·BF_4 revealed only one set of signals with the same desymetrization phenomena described above, indicating the exclusive formation of the chelate five-membered ring complex, probably owing to the proximity of the P-atom and of the potentially bridging μ-chloride. This assumption was further confirmed by an X-ray structure of **14**·BPh_4, prepared in a similar manner but containing the more crystallogenic tetraphenylborate anion (Figure 3).

The expected cyclic structure of the bimetallic cationic complex **14**·BPh_4 is observed, resulting from the chelation of the arene−chlororuthenium cation by the phosphorus atom and one of the two chlorides belonging to the dichlorotitanocene−phosphine moiety (Figure 3). Chelation results in the formation of a five-membered metallacyclic ring. It should be pointed out that due to a slight conformational difference, the two enantiomers observed in this structure cannot be related one to each other by an inversion center. Figure 4, which represents the overlay of these enantiomers (one of them being inverted for superimposition), shows that a main conformational difference is due to a rotation of ca. 45° of the

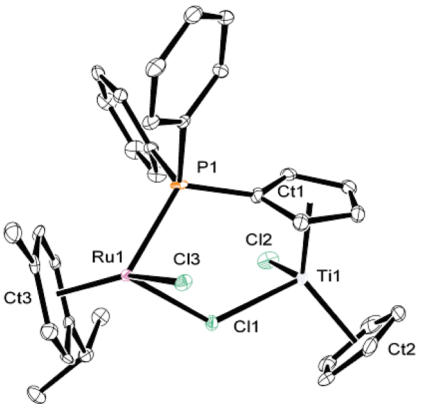

Figure 3. ORTEP view of the cation [(η^6-*p*-cymene)[(η^5-C_5H_5)(μ-η^5:κ^1-$C_5H_4PPh_2$)TiCl(μ-Cl)]RuCl] from **14**·BPh_4. Thermal ellipsoids are drawn at the 50% probability level. For clarity, only one enantiomer is shown and the tetraphenylborate anion is omitted. Selected bond lengths (Å) and angles (deg) (the second number refers to the second enantiomer) Ti1−Ct1 2.059(3), 2.061(3); Ti1−Ct2, 2.045(4), 2.046(4); Ti1−Cl1, 2.438(2), 2.448(2); Ti1−Cl2, 2.338(2), 2.339(2); Ru1−Ct3, 1.715(3), 1.724(3); Ru1−Cl1, 2.455(2), 2.443(2); Ru1−Cl3, 2.388(2), 2.391(2); Ru1−P1, 2.353(2), 2.343(2); Ct1−Ti1−Ct2, 131.1(14), 131.3(14); Cl1−Ti1−Cl2, 96.53(8), 95.09(8); Cl1−Ru1−Cl3, 88.31(6), 88.35(6); Cl1−Ru1−P1; 85.13(6), 83.94(6); Cl3−Ru1−P1, 87.28(6), 82.07(6); Ti1−Cl1−Ru1, 128.12(7), 128.35(7).

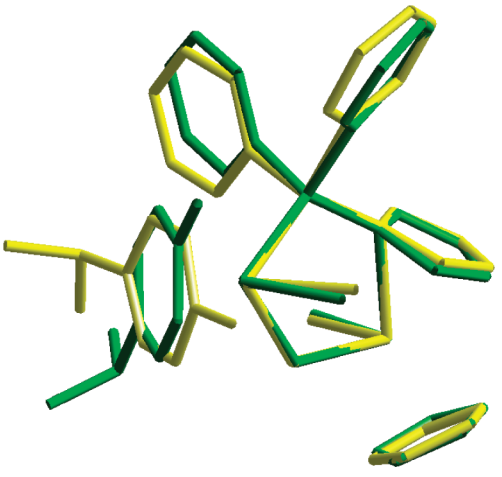

Figure 4. Overlay of the two independent cations (one being inverted) in **14**·BPh_4. A root-mean-square fit was performed on the five-membered rings to facilitate the superimposition of the two structures.

p-cymene ligand. Consequently, in the following general description of the geometrical parameters of **14**·BPh_4, two numbers are quoted. The titanocene moiety exhibits the expected geometry with, as expected, two different Ti−Cl bond lengths: 2.338(2), 2.340(2) Å for the terminal chloride ligand and a longer

Table 1. IC_{50} Values of **7**−**15** against Human Ovarian Carcinoma Cell Lines Sensitive (A2780) or Resistant (A2780cisR) and to Cisplatin and Inhibition Activity against Bovine cat B[a]

	cytotoxicity IC_{50} (μM)[b]		
compound	A2780	A2780cisR	cat B inhibition IC_{50} (μM)[b]
7	10.4 ± 1.1	5.9 ± 0.8	5 ± 1
8	6.8 ± 1.3	4.5 ± 1.1	15 ± 2
9	35.7 ± 2.9	28.7 ± 2.0	25 ± 3
10	28.3 ± 2.2	25.4 ± 1.7	> 50
11	11.1 ± 1.1	15.8 ± 1.7	35 ± 5
12	5.2 ± 1.3	5.4 ± 1.1	18 ± 5
13	15.7 ± 2.1	13.4 ± 2.0	20 ± 2
14	13.8 ± 1.9	8.7 ± 2.4	> 50
15	5.8 ± 1.6	7.1 ± 1.7	8 ± 2
2	80 ± 15	100 ± 18	25 ± 4
RAPTA-C	> 300	> 300	2.5 ± 0.5[c]
$Ti(\eta^5\text{-}C_5H_5)_2Cl_2$	570 ± 1.3[d]		17 ± 5
RAPTA-C + $Ti(\eta^5\text{-}C_5H_5)_2Cl_2$	> 200	> 200	

[a] RAPTA-C, Cp_2TiCl_2, titanocene-phosphine **2**, and compound **15** are reported for comparison. [b] Mean ± SE of at least three determinations. [c] Value taken from ref 18. [d] Value taken from ref 29.

one of 2.448(2), 2.448(2) Å for the μ-Cl ligand. The ruthenium moiety exhibits a distorted three-legged piano stool structure with two different Ru−Cl bonds: 2.388(2), 2.391 (2) Å for the terminal chloride ligand and a longer one of 2.455(2), 2.443(2) Å for the bridging ligand. The five-membered ring is almost planar, with a root-mean-square deviation to the mean plane of 0.13, 0.15 Å. The terminal chloride ligands are located in a *trans* position to each other with respect to this plane, the torsion angle Cl2−Ti−Ru-Cl3 being equal to −172.80(7), 169.04(7)°. The observed Ti···Ru intermetallic distance is 4.4008(13), 4.4018(12) Å.

The antiproliferative properties of **7**−**14** were assayed by monitoring their ability to inhibit cell growth using the MTT assay (see Experimental Section). Cytotoxic activity was determined on the human ovarian cancer (A2780) cell line, and its cisplatin-resistant variant (A2780cisR), after 72 h exposure to the compounds, in comparison to RAPTA-C and titanocene dichloride as controls. The obtained results are summarized in Table 1. Notably, all the compounds were active in the range of 4−36 μM and therefore markedly more cytotoxic than the reference compounds on both cell lines. The most effective compounds among the series are **12** ($IC_{50} \approx$ 5 μM), **7**, and **8** (IC_{50} in the range 4−10 μM). Notably, these compounds were more effective than cisplatin on the A2780cisR cell line, indicating lack of cross resistance and supporting the idea of a mechanism of action different to cisplatin.[27] It is noteworthy that the majority of the complexes were more cytotoxic toward the resistant cell line. Interestingly, coadministration of RAPTA-C and titanocene dichloride did not produce any significant cytotoxic effect on both cell lines, supporting the idea that the new dinuclear compounds possess peculiar chemicophysical properties with respect to their precursors responsible for the observed biological effects.

The complexes were also screened for inhibition of cat B using an established spectrophotomeric assay (see Experimental Section) in order to evaluate the affinity of the dinuclear compounds for the enzyme in comparison to RAPTA-C. It is worth mentioning that a compound that inhibits cat B is not necessarily a cytotoxic agent, as is the case of RAPTA-C,

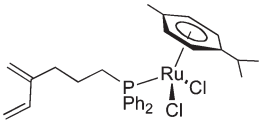

15

$[(\eta^6\text{-}p\text{-cymene})RuCl_2(\kappa^1\text{-}(CH_2{=}CH\text{-}C(=CH_2)(CH_2)_3PPh_2))]$

Figure 5. Structure of the model mononuclear Ru(II) compound **15**.

which is one of the most potent cat B inhibitors but is not cytotoxic. RAPTA-C prevents the progression of metastasis via a mechanism that probably involves inhibition of cat B in the extracellular matrix or associated with the plasma membrane. As mentioned above, however, inhibition of intracellular cat B may be involved in the induction of apoptotic pathways. In any case, inhibition of cat B by metal complexes can be envisaged in order for the compounds to exert an anticancer effect either cytotoxic or antimetastatic. Indeed, metal complexes are often good inhibitors of cat B and other cysteine proteases, which are therefore worth considering as potential targets.[28]

The obtained in vitro data for cat B inhibition are reported in Table 1, revealing that the different complexes inhibit cat B to varying degrees, the most effective inhibitor being **7**, with an IC_{50} value of about 5 μM, close to the value for RAPTA-C (IC_{50} = 2.5 ± 0.5 μM).[18] Notably, some preliminary structure−activity relationships could be drawn that correlate the inhibitory potency of the compounds with the alkyl chain in each complex. For example, the longer the chain the more effective the inhibitor (as can be observed among **7**, **8**/**12**, and **9**). In addition, the presence of secondary alkylaryl−phosphine ligands (**10**) appears to reduce the inhibition properties of the compound as well as the substitution of chlorides with fluorides in the Ti-ligand set (**11**). The cationic derivatives are less effective than their corresponding neutral precursors (**13** vs **8** and **14** vs **9**).

Examination of the inhibition of cat B by **7** over time revealed an exponential decay of enzyme activity (data not shown), indicating that a certain period of time is required to establish maximum inhibition, after which time no further inhibition is obtained. In the case of **7**, at least 9 h incubation at 25 °C were necessary to achieve the maximum inhibition; this effect might be due to the fact that initial hydrolysis of the metal complex, followed by covalent binding to cat B, is required for effective enzyme inhibition. These data are in good accordance with previously reported ones on RAPTA compounds.[18a]

Because the active site cysteine (Cys) of cat B was proposed to be the anchoring site for the ruthenium(II) center upon RAPTA complexes binding,[18a] we hypothesized a similar mechanism of inhibition for the bimetallic compounds, although the Ti ion could also compete for binding with the Cys.

To assess the importance of each metal center (Ti or Ru) for cat B inhibition, the model compounds $[(\eta^6\text{-}p\text{-cymene})RuCl_2(\kappa^1\text{-}(CH_2{=}CH\text{-}C(=CH_2)(CH_2)_3PPh_2))]$ **15** and $[(\eta^5\text{-}C_5H_5)(\eta^5\text{-}C_5H_4(CH_2)_2PPh_2)TiCl_2]$ **2** were also screened (Figure 5, Scheme 1, Table 1). It was not possible to prepare the complex $[(\eta^6\text{-}p\text{-cymene})[(\kappa^1\text{-}C_5H_5(CH_2)_4PPh_2]RuCl_2]$ because of oligomerization of the cyclopentadiene part through Diels−Alder reaction, and therefore **15** is a good compromise as a model of mononuclear precursor of **7**. Interestingly, **15** is a relatively good inhibitor ($IC_{50} \sim 8$ μM), supporting the notion that the Ru moiety is essential for the compound to interact

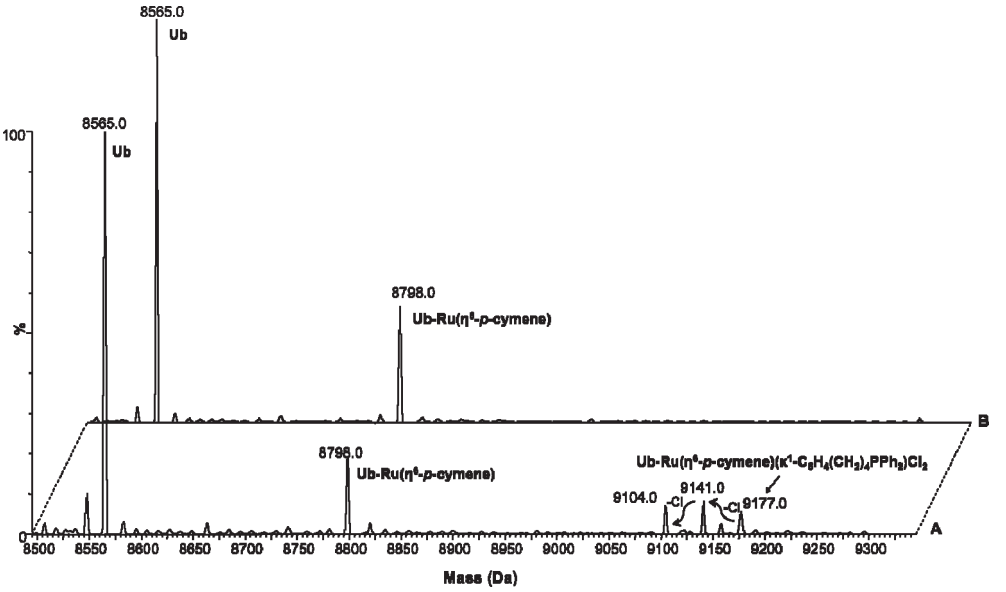

Figure 6. Deconvoluted ESI-MS spectra of Ub incubated with **7** (metal complex:Ub ratio = 3:1) for (A) 3 and (B) 24 h at 37 °C.

with the cat B active site, whereas **2** is less effective (IC_{50} about 25 μM). Because the cytotoxicity of **15** is equivalent to the bimetallic derivatives, the role of the phosphine ligand on the biological effects of the bimetallic compounds cannot be excluded. Similarly, **2** (IC_{50} = 80−100 μM) resulted in being more cytotoxic than titanocene dichloride.

The cat B structure is roughly disk-shaped and shows a marked incision corresponding to the active site cleft.[30] The peptide chain is folded into two distinct domains, which interact with one another through an extended polar interface which opens to the V-shaped active site cleft. Near the active site are two main interaction site pockets, a large hydrophobic one and a smaller one, which is more accessible to solvent. In the case of the reported bimetallic compounds, the length of the spacer between the titanocene group and the ruthenium−arene moiety influences the reactivity of compound, the most elongated chains favoring the penetration of the Ru(II) center in the protein active site cavity until it reaches the catalytic Cys. In addition, beyond the coordinative bond of Ru(II) to the sulfur of the Cys residue, a number of contacts of the alkyl chain and the phosphine group could be also established within the protein active site cavity as it has been hypothesized for the typical ligand set of RAPTA compounds.[18a]

To better characterize the interaction of the bimetallic complexes with proteins, the reactivity of **7** with two model proteins, ubiquitin (Ub) and human carbonic anhydrase II (hCAII), was studied using electrospray ionization mass spectrometry (ESI-MS). The use of a model system was necessary since our attempts to obtain well resolved cat B mass spectra were unsuccessful. It is worth noting that Ub was selected as a model system because it is particularly amenable to MS analysis:[31] it has favorable properties such as moderate size (M_w of ca. 8500 Da) and a high stability in solution under physiological-like conditions. hCAII is a zinc metalloenzyme (M_W of ca. 29 KDa) and was selected because it contains a surface exposed Cys residue that might have affinity for binding to the bimetallic Ti−Ru complexes as anticipated for the Cys residue in the cat B active site. In a typical experiment, 3 molar equivalents of **7** were added to an aqueous solution of each protein buffered at pH 7.4 and the mixture was maintained at 37 °C until analysis. Figure 6 shows the deconvoluted mass spectra obtained at two different time intervals for Ub. Ub was identified as one of the main peaks at 8565 Da, and after 3 h, adducts of **7** were identified at 8798 and at 9177 Da corresponding to protein bound [Ru(η^6-*p*-cymene)] and [(η^6-*p*-cymene)($C_5H_5(CH_2)_4PPh_2$)$RuCl_2$] fragments, respectively. After 24 h, only the adduct bearing the [Ru(η^6-*p*-cymene)] fragment is present; similar results were obtained with the other complexes. It is worth noting that in all cases the titanium moiety has been released from the original complex, suggesting that cleavage of the titanium ion also takes place on binding to cat B, although the influence of the ionization process on fragmentation of the complex cannot be ruled out.

When the same experiment was repeated with hCAII, similar reactivity profiles were observed. Representative spectra recorded after incubation with **7** for 24 h are shown in Figure 7. Notably, a hCAII-adduct is observed (M_w of ca. 29817 Da), most likely bearing a [(η^6-*p*-cymene)[(μ-η^5:κ^1-$C_5H_4(CH_2)_4PPh_2$)Ti]$RuCl_2$] fragment, supporting the hypothesis that the Ti ion also plays a role in the biological mechanism of the compounds.

Conclusions

Organometallic compounds are currently attracting considerable attention as putative anticancer agents that offer properties intermediate between those of classical inorganic (coordination) complexes and organic drug molecules.[5,32] Herein, a series of titanocene−ruthenium bimetallic complexes have been synthesized and characterized. The X-ray structure obtained for the unprecedented cationic bimetallic complex revealed a chelate structure involving a bridging chloride ligand between the two metal centers.

All the compounds were screened for their cytotoxicity against selected cancer cell lines and were found to be considerably more active than their parent mononuclear titanocene dichloride and Ru−arene precursors. The compounds were also more cytotoxic than cisplatin in the resistant cell line. Moreover, some of them showed relevant cat B inhibition properties in vitro that correlate to some extent with the observed antiproliferative effects. Consequently, we can hypothesize that inhibition of cysteine proteases such as cat B could account to some extent for the biological effects of

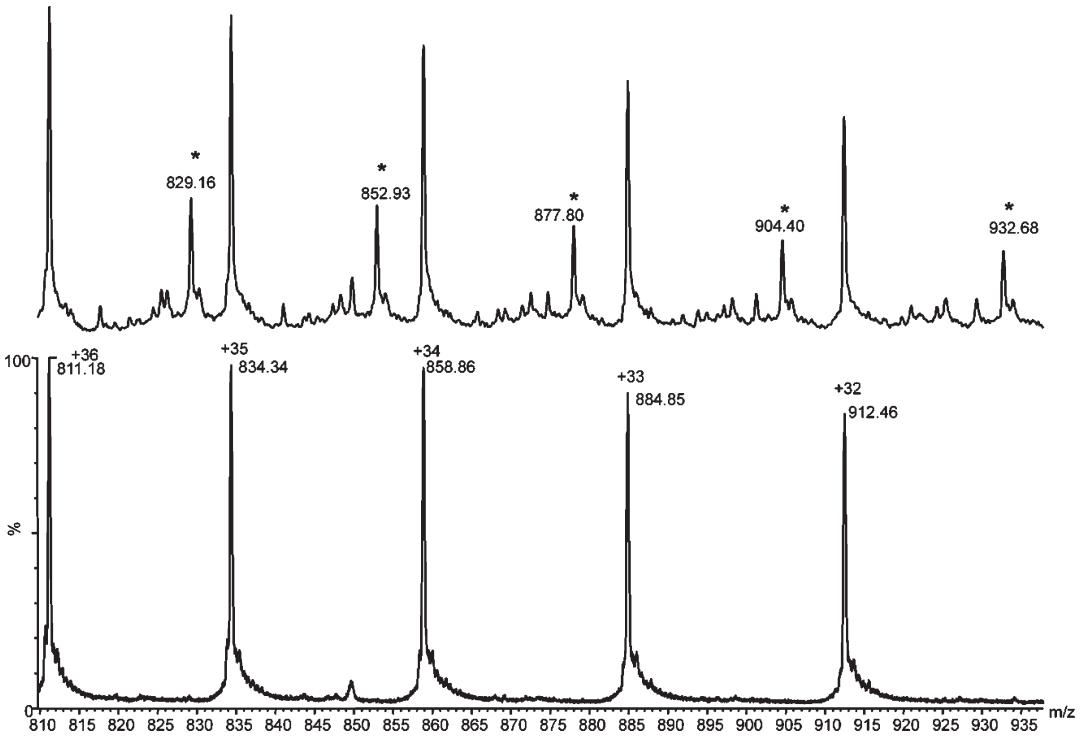

Figure 7. ESI-MS spectra of hCAII (bottom) and hCAII incubated with **7** (top) (metal complex:hCAII ratio = 3:1) for 24 h at 37 °C. * = [(η^6-*p*-cymene)[(μ-η^5:κ^1-$C_5H_4(CH_2)_4PPh_2$)Ti]$RuCl_2$].

the reported compounds. However, it should be noted that inhibition of cysteine cathepsins might occur either extracellularly or intracellularly and that other studies are necessary to clarify all the relevant targets of these compounds. Nevertheless, cysteine proteases are an important class of target for metal-based drugs.[29]

For the Ti−Ru complexes, cat B binding probably occurs through the interaction of the Ru center with the catalytic Cys residue, which is facilitated in the case of complexes bearing longer alkyl chains between the two metal ions. This mechanistic hypothesis is supported by the fact that the Ru precursor (**15**) bearing a phosphine similar to the ones used as linkers is a more active cat B inhibitor than the titanocene−phosphine derivative (**2**). It is worth mentioning that both the mononuclear derivatives **2** and **15** demonstrated an enhanced cytotoxic effect compared to titanocene dichloride and RAPTA-C, respectively. This effect might be related to improved stability, solubility, or lipophilicity properties of the compounds induced by the phosphine moiety.

Finally, complementary information obtained by ESI-MS analysis of the complexes following incubation with Ub and hCAII provided evidence of the binding of Ru-containing species to the peptides, and in the case of hCAII, binding of a bimetallic species is observed.

The reported results indicate that this family of heteronuclear complexes possesses antiproliferative properties that operates via a different pharmacological mechanism with respect to titanocene dichloride and to RAPTA compounds, exemplified by RAPTA-C, which displays good cat B inhibition yet limited cytotoxicity, although significant activity against solid metastasis in vivo.[10] A similar correlation between cytotoxicity and cat B inhibition has been recently described for dinuclear Pd complexes.[33]

Experimental Section

General Remarks. All reactions were carried out under an atmosphere of purified argon using Schlenk techniques. Solvents were dried and distilled under argon before use. The complexes [(η^5-C_5H_5)(η^5-$C_5H_4(CH_2)_2PPh_2$)$TiCl_2$] (**2**),[34] [(η^5-C_5H_5)-(η^5-$C_5H_4PPh_2$)$TiCl_2$] (**3**),[25a] [(η^5-C_5H_5)(η^5-$C_5H_4(CH_2)_2PPh_2$)-TiF_2] (**5**),[25b] and [(η^5-C_5H_5)(η^5-$C_5H_4(CH_2)_2PCy_2$)$TiCl_2$] (**6**),[25c] and the corresponding ruthenium-complexes [(η^6-*p*-cymene)-[(η^5-C_5H_5)(μ-η^5:κ^1-$C_5H_4(CH_2)_2PPh_2$)$TiCl_2$]$RuCl_2$] (**8**),[25a] [(η^6-*p*-cymene)[(η^5-C_5H_5)(μ-η^5:κ^1-$C_5H_4PPh_2$)$TiCl_2$]$RuCl_2$] (**9**),[25a] [(η^6-*p*-cymene)[(η^5-C_5H_5)(μ-η^5:κ^1-$C_5H_4(CH_2)_2PPh_2$)TiF_2]$RuCl_2$] (**11**),[25b] and [(η^6-*p*-cymene)[(η^5-C_5H_5)(μ-η^5:κ^1-$C_5H_4(CH_2)_2PCy_2$)-$TiCl_2$]$RuCl_2$] (**12**)[25c] were synthesized according to literature procedures. The detailed synthesis and characterization of the model compound **15** will be reported elsewhere.[35] The high thermal instability of (4-bromobutyl)cylopenta-1,3-diene, even at room temperature, and the moisture sensitivity of the lithium cyclopentadienides Li[$C_5H_4(CH_2)_4PPh_2$] and Li[$C_5H_4C(CH_3)_2$-P(H)Ph] excluded their complete spectroscopic characterization. Nevertheless, they were used for the synthesis of bimetallic complexes **1** and **4**. All other reagents were commercially available and used as received. All the analyses were performed at the "Plateforme d'Analyses Chimiques et de Synthèse Moléculaire de l'Université de Bourgogne". The identity and purity (≥95%) of the complexes were unambiguously established using elemental analysis, high-resolution mass spectrometry, and NMR. Elemental analyses were obtained on an EA 1108 CHNS-O FISONS Instrument. Exact mass of the synthesized bimetallic complexes were obtained on a Bruker micrOTOF-Q ESI-MS. ^{1}H (500.13 or 600.13 MHz) and ^{31}P (202.5 or 242.9 MHz) NMR spectra were recorded on a Bruker 500 Avance DRX spectrometer or on a Bruker 600 Avance II spectrometer. Chemical shifts are quoted in ppm (δ) relative to TMS (^{1}H), using the residual protonated solvent as internal standard, or external 85% H_3PO_4 (^{31}P). Coupling constants are reported in Hertz.

Synthesis. (4-Bromobutyl)cylopenta-1,3-diene, [$C_5H_5(CH_2)_4Br$] (Mixture of 1- and 2-Substituted Isomers). Sodium cylopentadienide (33.2 g, 377 mmol) in THF (120 mL) were added dropwise to a solution of 1,4-dibromobutane (45 mL, 376 mmol) in THF (50 mL) at 0 °C. The mixture was then warmed to room temperature and stirred for 12 h. The resulting mixture was treated with water (30 mL) and the product extracted with dichloromethane

(150 mL). The solution was concentrated under reduced pressure and the pale-yellow residue was distillated (bp = 64 °C, 1 mmHg). The compound was obtained spectroscopically pure in 20% yield (4.60 g) although it was found to be highly unstable due to autocondensation through Diels−Alder reactions when stored neat at room temperature. 1-(4-Bromobutyl)cylopenta-1,3-diene (minor isomer, 45%): ^{1}H NMR ($CDCl_3$) δ 1.73 (m, 2H, CH_2), 1.92 (m, 2H, CH_2), 2.43 (m, 2H, CH_2), 2.91 (m, 2H, C_5H_5), 3.45 (t, 2H, CH_2, $^3J_{HH}$ = 6.7 Hz), 6.21 (m, 1H, C_5H_5), 6.30 (m, 1H, C_5H_5), 6.46 (m, 1H, C_5H_5); ^{13}C{^{1}H} NMR ($CDCl_3$) δ 27.3, 28.1, 29.8, 32.5 (*C*H_2), 43.2, 126.8, 130.7, 132.4, 148.9 (*C*$_5H_5$). 2-(4-Bromobutyl)cylopenta-1,3-diene (major isomer, 55%): ^{1}H NMR ($CDCl_3$) δ 1.73 (m, 2H, CH_2), 1.92 (m, 2H, CH_2), 2.50 (m, 2H, CH_2), 2.99 (m, 2H, C_5H_5), 3.45 (t, 2H, CH_2, $^3J_{HH}$ = 6.7 Hz), 6.06 (m, 1H, C_5H_5), 6.46 (m, 2H, C_5H_5); ^{13}C{^{1}H} NMR ($CDCl_3$) δ 27.3, 28.9, 32.4, 33.8 (*C*H_2), 41.3, 126.3, 133.9, 134.5, 146.4 (*C*$_5H_5$).

Lithium (4-Diphenylphosphinobutyl)cyclopentadienide, Li[C_5H_4-(CH_2)$_4$$PPh_2$]. A solution of $LiPPh_2$ (2.58 g, 13.43 mmol) in THF (20 mL) was added dropwise to a solution of $C_5H_5(CH_2)_4Br$ (4.18 g, 20.78 mmol) in THF (40 mL) at −40 °C. The solution was warmed to room temperature and stirred for 12 h. The solvent was removed under reduced pressure, and the product was extracted with *n*-pentane (50 mL). The solution was filtered on a sintered funnel, and *n*-butyllithium was added (1.6 M in hexanes, 8.4 mL, 13.43 mmol) at 0 °C. The precipitate was collected on a sintered funnel and dried under reduced pressure to afford a white powder (2.82 g, 67% yield). ^{31}P{^{1}H} NMR (THF/C_6D_6 capillary) δ −13.1 (s, PPh_2).

Lithium (1-Methyl-1-phenylphosphino)ethylcyclopentadienide, Li[$C_5H_4C(CH_3)_2P(H)Ph$]. This compound was synthesized by a modified literature procedure.[26] To a solution of $PhPH_2$ (0.91 M in hexanes, 6 mL, 5.46 mmol) in THF (20 mL) at −78 °C, *n*-butyllithium (1.4 M in hexanes, 3.9 mL, 5.5 mmol) was slowly added. After 1 h stirring at this temperature, a solution of dimethylfulvene (580 mg, 5.5 mmol) in THF (15 mL) was added to the formed phenylphosphide yellow suspension at −78 °C. The resulting orange clear solution was warmed to room temperature and stirred for a further 48 h. After evaporation of the solvent and precipitation with *n*-pentane, the solution was filtered and the solid washed with *n*-pentane (2 × 15 mL). The cyclopentadienide was dried under vacuum at room temperature to afford an off-white powder (855 mg, 70% yield). ^{31}P NMR (THF/C_6D_6 capillary) δ 0.1 (d, $^1J_{PH}$ = 206 Hz, *P*PhH).

[(η^5-C_5H_5)(η^5-$C_5H_4(CH_2)_4PPh_2$)$TiCl_2$] (1). A solution of [$C_5H_4(CH_2)_4PPh_2$]Li (387 mg, 1.24 mmol) in THF (10 mL) was added dropwise at 0 °C to a solution of [(η^5-C_5H_5)$TiCl_3$] (272 mg, 1.24 mmol) in THF (15 mL). The red solution was stirred for 4 h at room temperature. The solvent was removed under reduced pressure, and dichloromethane (30 mL) was added. The mixture was filtered, and *n*-hexane (40 mL) was added to the solution to form a biphasic solution that was stored at 4 °C. Red crystals were obtained and collected (365 mg, 60% yield). ^{31}P{^{1}H} NMR ($CDCl_3$) δ −15.2 (s, *P*Ph_2). ^{1}H NMR ($CDCl_3$) δ 1.48 (m, 2H, CH_2), 1.71 (m, 2H, CH_2), 2.06 (m, 2H, CH_2), 2.71 (m, 2H, CH_2), 6.28 (m, 2H, C_5H_4), 6.39 (m, 2H, C_5H_4), 6.53 (s, 5H, Cp), 7.31−7.34 (m, 6H, Ph), 7.37−7.40 (m, 4H, Ph).

[(η^5-C_5H_5)(η^5-$C_5H_4(CMe_2)P(H)Ph$)$TiCl_2$] (4). To a solution of [(η^5-C_5H_5)$TiCl_3$] (775 mg, 3.53 mmol) in THF (10 mL) at 0 °C a solution of lithium (1-methyl-1-phenylphosphino)ethylcyclopentadienide (827 mg, 3.72 mmol) in THF (10 mL) was added dropwise. The deep-red solution immediately obtained was stirred for 4 h at room temperature. After evaporation of the THF under reduced pressure, addition of toluene ensured the precipitation of LiCl which was removed by filtration. Evaporation of toluene under reduced pressure afforded a red powder that was further purified by addition of CH_2Cl_2 (30 mL) and precipitation following the addition of *n*-hexane (60 mL). After filtration on a sintered funnel, the solid was dried under vacuum to afford a red powder (764 mg, 54% yield). ^{31}P NMR (C_6D_6) δ 17.4 (d, $^1J_{PH}$ = 208 Hz, *P*PhH). ^{1}H NMR (C_6D_6) δ 1.76 (d, 3H, C(CH_3)$_2$, $^4J_{PH}$ = 15.0 Hz), 1.82 (d, 3H, C(CH_3)$_2$, $^3J_{PH}$ = 14.4 Hz), 4.07 (d, 1H, P-*H*, $^1J_{PH}$ = 208 Hz), 5.71 (m, 1H, C_5H_4), 5.84 (m, 2H, C_5H_4), 6.07 (s, 5H, Cp), 6.15 (m, 1H, C_5H_4), 7.07−7.21 (m, 5H, Ph).

[(η^6-*p*-Cymene)[(η^5-C_5H_5)(μ−η^5:κ^1-$C_5H_4(CH_2)_4PPh_2$)$TiCl_2$]-$RuCl_2$] (7). A solution of [(η^5-C_5H_5)(η^5-$C_5H_4(CH_2)_4PPh_2$)$TiCl_2$] (**1**) (93 mg, 0.19 mmol) and [(η^6-*p*-cymene)$RuCl_2$]$_2$ (52 mg, 0.17 mmol) in degassed benzene (5 mL) was stirred at room temperature for 4 h. An orange−red precipitate slowly appeared. The solid was filtered on a sintered funnel and dried under vacuum to afford an orange−red powder (128 mg, 95% yield). Red crystals suitable for X-ray diffraction were grown from CH_2Cl_2/*n*-hexane (1/3). ^{31}P{^{1}H} NMR ($CDCl_3$) δ 23.6 (s, *P*Ph_2). ^{1}H NMR ($CDCl_3$) δ 0.82 (d, 6H, CH(CH_3)$_2$, $^3J_{HH}$ = 7.0 Hz), 1.10 (m, 2H, CH_2), 1.42 (m, 2H, CH_2), 1.91 (s, 3H, CH_3 *p*-cymene), 2.48 (m, 2H, CH_2), 2.54 (hept, 1H, CH(CH_3)$_2$, $^3J_{HH}$ = 7.0 Hz), 2.56 (m, 2H, CH_2), 5.10 (d, 2H, =C*H* *p*-cymene, $^3J_{HH}$ = 6.0 Hz), 5.28 (d, 2H, =C*H* *p*-cymene, $^3J_{HH}$ = 6.5 Hz), 6.23 (m, 2H, C_5H_4), 6.35 (m, 2H, C_5H_4), 6.54 (s, 5H, Cp), 7.39−7.53 (m, 6H, Ph), 7.86−7.90 (m, 4H, Ph). Anal. Calcd for $C_{36}H_{41}Cl_4PTiRu$ (795.43): C; 54.36, H; 5.20. Found: C; 54.55, H; 5.20.

[(η^6-*p*-Cymene)[(η^5-C_5H_5)(μ-η^5:κ^1-$C_5H_4(CMe_2)P(H)Ph$)$TiCl_2$]-$RuCl_2$] (10). A solution of [(η^5-C_5H_5)(η^5-$C_5H_4(CMe_2)P(H)Ph$)$TiCl_2$] (**4**) (73 mg, 0.18 mmol) and [(η^6-*p*-cymene)$RuCl_2$]$_2$ (51 mg, 0.16 mmol) in degassed benzene (5 mL) was stirred at room temperature for 4 h, during which time a mauve precipitate formed. The solid was removed by filtration and dried under vacuum to afford a mauve powder (110 mg, 95% yield). ^{31}P NMR ($CDCl_3$) δ 59.8 (d, $^1J_{PH}$ = 380 Hz, *P*PhH). ^{1}H NMR ($CDCl_3$) δ 1.04 (d, 3H, CH(CH_3)$_2$, $^3J_{HH}$ = 7.0 Hz), 1.19 (d, 3H, CH(CH_3)$_2$, $^3J_{HH}$ = 7.0 Hz), 1.80 (d, 3H, C(CH_3)$_2$, $^4J_{PH}$ = 16.2 Hz), 1.94 (d, 3H, C(CH_3)$_2$, $^3J_{PH}$ = 16.8 Hz), 2.04 (s, 3H, CH_3 *p*-cymene), 2.81 (hept, 1H, CH(CH_3)$_2$, $^3J_{HH}$ = 7.0 Hz), 5.23 (d, 1H, =C*H* *p*-cymene, $^3J_{HH}$ = 5.7 Hz), 5.41 (d, 1H, =C*H* *p*-cymene, $^3J_{HH}$ = 5.7 Hz), 5.48 (d, 1H, P-*H*, $^1J_{PH}$ = 380 Hz), 5.55 (m, 2H, =C*H* *p*-cymene), 6.25 (m, 1H, C_5H_4), 6.41 (m, 1H, C_5H_4), 6.49 (m, 1H, C_5H_4), 6.56 (s, 5H, Cp), 6.58 (m, 1H, C_5H_4), 7.22−7.34 (m, 5H, Ph). ESI-MS (CH_2Cl_2/CH_3CN, positive mode) *exact mass* for $C_{29}H_{35}Cl_4PTiRu$ (703.97535): found *m*/*z* 669.00894 [M − Cl]$^+$ (calcd *m*/*z* 669.00594).

[(η^6-*p*-Cymene)[(η^5-C_5H_5)(μ-η^5:κ^1-$C_5H_4(CH_2)_2PPh_2$)$TiCl_2$]-RuCl](BF_4). A suspension of (η^6-*p*-cymene)[(η^5-C_5H_5)(μ-η^5:κ^1-$C_5H_4(CH_2)_2PPh_2$)$TiCl_2$]$RuCl_2$ (**8**) (278 mg, 0.36 mmol) and $AgBF_4$ (85 mg, 0.43 mmol) in dichloromethane (10 mL) was stirred in the dark at room temperature for 4 h. The color of the mixture turned violet. The silver chloride precipitate was removed by filtration and the solvent was removed under vacuum. The red−brown powder was washed with Et_2O (2 × 5 mL) and dried under vacuum (182 mg, 62% yield). ESI-MS (CH_2Cl_2/MeOH, positive mode) *exact mass* for $C_{34}H_{37}Cl_3PRuTi$ (731.02214): found *m*/*z* 769.05782 [M − H + K]$^+$ (calcd *m*/*z* 768.97802).

Major Isomer [(η^6-*p*-Cymene)[(η^5-C_5H_5)(μ-η^5:κ^1-$C_5H_4(CH_2)_2$-PPh_2)$TiCl_2$]RuCl](BF_4) (13′·BF_4). ^{31}P{^{1}H} NMR (CD_2Cl_2) δ 23.3 (s, *P*Ph_2). ^{1}H NMR (CD_2Cl_2) δ 0.90 (d, 3H, CH(CH_3)$_2$, $^3J_{HH}$ = 6.6 Hz), 0.93 (d, 3H, CH(CH_3)$_2$, $^3J_{HH}$ = 6.6 Hz), 1.95 (s, 3H, CH_3 *p*-cymene), 2.44−2.48 (m, 3H, CH(CH_3)$_2$ + CH_2), 2.74−2.79 (m, 2H, CH_2), 5.25 (m, 2H, =C*H* *p*-cymene), 5.40 (m, 2H, =C*H* *p*-cymene), 6.26 (m, 2H, C_5H_4), 6.38 (m, 2H, C_5H_4), 6.49 (s, 5H, Cp), 7.58−7.60 (m, 6H, Ph), 7.84−7.89 (m, 4H, Ph).

Minor Isomer [(η^6-*p*-Cymene)[(η^5-C_5H_5)(μ-η^5:κ^1-$C_5H_4(CH_2)_2$-PPh_2)$TiCl$(μ-Cl)]$RuCl$](BF_4) (13·BF_4). ^{31}P{^{1}H} NMR (CD_2Cl_2) δ 23.2 (s, *P*Ph_2). ^{1}H NMR (CD_2Cl_2) δ 0.86 (d, 3H, CH(CH_3)$_2$, $^3J_{HH}$ = 7.2 Hz), 0.90 (d, 3H, CH(CH_3)$_2$, $^3J_{HH}$ = 7.2 Hz), 1.95 (s, 3H, CH_3 *p*-cymene), 2.32 (m, 1H, CH(CH_3)$_2$), 2.54−2.57 (m, 2H, CH_2), 2.68−2.73 (m, 2H, CH_2), 5.21 (m, 1H, =C*H* *p*-cymene), 5.28 (m, 1H, =C*H* *p*-cymene), 5.38 (m, 1H, =C*H* *p*-cymene), 5.43 (m, 1H, =C*H* *p*-cymene), 6.13 (m, 1H, C_5H_4), 6.19 (m, 1H, C_5H_4),

6.28 (m, 1H, C_5H_4), 6.52 (s, 5H, Cp), 6.69 (m, 1H, C_5H_4), 7.58−7.60 (m, 6H, Ph), 7.84−7.89 (m, 4H, Ph).

[(η^6-*p*-Cymene)[(η^5-C_5H_5)(μ-η^5:κ^1-$C_5H_4PPh_2$)TiCl(μ-Cl)]RuCl]-(BF_4) (14·BF_4). The same procedure used for **13**·BF_4 was applied using [(η^6-*p*-cymene)[(η^5-C_5H_5)(μ-η^5:κ^1-$C_5H_4PPh_2$)$TiCl_2$]$RuCl_2$] (**9**) (153 mg, 0.208 mmol) and $AgBF_4$ (49 mg, 0.249 mmol) to afford the product as a red−brown powder (123 mg, 75% yield). $^{31}P\{^1H\}$ NMR (CD_2Cl_2) δ 33.3 (s, *P*Ph_2). ^1H NMR (CD_2Cl_2) δ 1.34 (d, 3H, CH(CH_3)$_2$, $^3J_{HH}$ = 7.0 Hz), 1.37 (d, 3H, CH(CH_3)$_2$, $^3J_{HH}$ = 7.0 Hz), 1.84 (s, 3H, CH_3 *p*-cymene), 2.83 (hept, 1H, C*H*(CH_3)$_2$, $^3J_{HH}$ = 7.0 Hz), 5.07 (d, 1H, =C*H* *p*-cymene, $^3J_{HH}$ = 7.0 Hz), 5.45 (d, 1H, =C*H* *p*-cymene, $^3J_{HH}$ = 7.0 Hz), 5.51 (d, 1H, =C*H* *p*-cymene, $^3J_{HH}$ = 7.0 Hz), 5.52 (m, 1H, C_5H_4), 5.85 (d, 1H, =C*H* *p*-cymene, $^3J_{HH}$ = 7.0 Hz), 6.65−6.72 (m, 2H, C_5H_4), 6.83 (s, 5H, Cp), 7.27 (m, 1H, C_5H_4), 7.30−7.85 (m, 10H, Ph). Anal. Calcd for $C_{32}H_{33}BCl_3F_4PTiRu$ (790.68): C; 48.61, H; 4.21. Found: C; 47.78, H; 4.28.

[(η^6-*p*-Cymene)[(η^5-C_5H_5)(μ-η^5:κ^1-$C_5H_4PPh_2$)TiCl(μ-Cl)-]RuCl](BPh_4) (14·BPh_4). The same procedure used for **13**.BPh_4 was applied using [(η^6-*p*-cymene)[(η^5-C_5H_5)(μ-η^5:κ^1-$C_5H_4PPh_2$)-$TiCl_2$]$RuCl_2$] (**9**) (153 mg, 0.208 mmol) and $AgBPh_4$ (78.3 mg, 0.249 mmol) to afford the product as a red−brown powder (138 mg, 65% yield). $^{31}P\{^1H\}$ NMR (CD_2Cl_2) δ 33.0 (s, *P*Ph_2). ^1H NMR (CD_2Cl_2) δ 1.32 (d, 3H, CH(CH_3)$_2$, $^3J_{HH}$ = 7.0 Hz), 1.36 (d, 3H, CH(CH_3)$_2$, $^3J_{HH}$ = 7.0 Hz), 1.75 (s, 3H, CH_3 *p*-cymene), 2.81 (hept, 1H, C*H*(CH_3)$_2$, $^3J_{HH}$ = 7.0 Hz), 4.92 (d, 1H, =C*H* *p*-cymene, $^3J_{HH}$ = 5.3 Hz), 5.32 (d, 1H, =C*H* *p*-cymene, $^3J_{HH}$ = 6.2 Hz), 5.42 (d, 1H, =C*H* *p*-cymene, $^3J_{HH}$ = 6.2 Hz), 5.70 (m, 1H, C_5H_4), 5.80 (d, 1H, =C*H* *p*-cymene, $^3J_{HH}$ = 5.3 Hz), 6.65 (s, 5H, Cp), 6.70 (m, 1H, C_5H_4), 6.85−7.15 (m, 12H, Ph + C_5H_4), 7.25−7.85 (m, 20H, Ph). Anal. Calcd for $C_{56}H_{53}BCl_3PTiRu$ (1023.1): C; 65.74, H; 5.22. Found: C; 65.36, H; 5.29.

X-ray Diffraction Analysis of 7 and 14·BPh_4. X-ray intensity data were collected at 115 K on a Bruker Nonius ApexII CCD system using graphite-monochromated Mo Kα radiation. The structures were solved by direct methods (SIR92)[36] and refined with full-matrix least-squares methods based on F^2 (SHELXL-97)[37] with the aid of the WINGX program.[38] Except for a disordered dichloromethane molecule in **7**, all non-hydrogen atoms were refined with anisotropic thermal parameters. Hydrogen atoms were included in their calculated positions and refined with a riding model. For **7**, dichloromethane solvate molecules were located in a channel along the 1/2, 1/2, *z* direction, which could explain why crystals are very unstable when isolated from the mother solution; even protected in paratone oil they rapidly loose solvent. Nevertheless, data could be recorded at low temperature. Two dichloromethane molecules in the solvate channel were located with partial occupations. One was anisotropically refined with an occupation factor of 0.57, while the second, located near an inversion center, was refined as a rigid group with an overall isotropic temperature factor and an occupation factor of 0.30. Furthermore, careful inspection of the anisotropic displacement parameters of the atoms belonging to **7** suggests a possible disorder of the overall molecule, but attempts to model this disorder did not lead to satisfactory results.

Cell Culture and Inhibition of Cell Growth. Human A2780 and A2780cisR ovarian carcinoma cell lines were obtained from the European Centre of Cell Cultures (ECACC, Salisbury, U.K.) and maintained in culture as described by the provider. The cells were routinely grown in RPMI 1640 medium containing 10% fetal calf serum (FCS) and antibiotics at 37 °C and 6% CO_2. For evaluation of growth inhibition tests, the cells were seeded in 96-well plates (Costar, Integra Biosciences, Cambridge, MA) and grown for 24 h in complete medium. The stock solutions of **7**−**14** were prepared by dissolving the compounds in 1 mL of DMSO to reach a concentration of 10^{-2} M. They were then diluted in RPMI medium and added to the wells (100 μL) to obtain a final concentration ranging between 0 and 80 μM. DMSO at comparable concentrations did not show any effects on cell cytotoxicity. Complexes **7**−**14** were diluted directly in culture medium to the required concentration and added to the cell culture. After 72 h incubation at 37 °C, 20 μL of a solution of MTT (3-(4,5-dimethylthiazole-2-yl)-2,5-diphenyltetrazolium bromide) in PBS (2 mg mL^{-1}) was added to each well, and the plates were then incubated for 2 h at 37 °C. The medium was then aspirated, and DMSO (100 μL) was added to dissolve the precipitate. The absorbance of each well was measured at 580 nm using a 96-well multiwell-plate reader (iEMS Reader MF, Labsystems, Bioconcept, Switzerland) and compared to the values of control cells incubated without complexes. The IC_{50} values for the inhibition of cell growth were determined by fitting the plot of the percentage of surviving cells against the drug concentration using a sigmoidal function (Origin v7.5).

Inhibition of Cathepsin B. Crude bovine spleen cat B was purchased from Sigma (C6286) and used without further purification. The colorimetric cat B assay was performed in 100 mM sodium phosphate, 1 mM EDTA, 0.025% BRIJ, pH 6.0, using Na-CBZ-L-lysine *p*-nitrophenyl ester (CBZ = *N*-carbobenzoxy) as substrate. For the enzyme to be catalytically functional, the active site cysteine needs to be in a reduced form. Therefore, prior to use, cat B was prereduced with dithiothreitol (DTT) to ensure that the majority of the enzyme is in a catalytically active form. Cat B was activated, before dilution, in the presence of excess DTT for 1 h at 30 °C. IC_{50} determinations were performed in triplicate using a fixed enzyme concentration, of 1 μM, and a fixed substrate concentration of 200 μM. Compound concentrations ranged from 0.3 to 300 μM. The enzyme and compound were coincubated at 25 °C for 24 h prior to the addition of substrate. Activity was measured over 2 min at 326 nm.

ESI-MS. Samples were prepared by mixing 100 μM Ub or hCAII (Sigma, U6253 and C6165, respectively) with an excess of metal complex (3:1, metal:protein ratio) in 20 mM $(NH_4)_2CO_3$ buffer (pH 7.4) and incubated for 24 h at 37 °C. Prior to analysis, samples were extensively ultrafiltered using a Centricon YM-3 filter (Amicon Bioseparations, Millipore Corporation) in order to remove the unbound complex. ESI-MS data were acquired on a Q-Tof Ultima mass spectrometer (Waters) fitted with a standard Z-spray ion source and operated in the positive ionization mode. Experimental parameters were set as follows: capillary voltage 3.5 kV, source temperature 80 °C, desolvation temperature 120 °C, sample cone voltage 100 V, desolvation gas flow 400 L/h, acquisition window 300−2000 *m*/*z* in 1 s. The samples were diluted 1:20 in water and 5 μL was introduced into the mass spectrometer by infusion at a flow rate of 20 μL/min with a solution of ACN/H_2O/HCOOH 50:49.8:0.2 (v:v:v). External calibration was carried out with a solution of phosphoric acid at 0.01%. Data were processed using the MassLynx 4.1 software.

Acknowledgment. We thank COST D39 action for stimulating discussions. A.C. thanks the Swiss National Science Foundation (AMBIZIONE project no. PZ00P2_121933) and the Swiss Confederation (Action COST D39−Accord de Recherche−SER project no. C09.0027) for financial support. M.P. thanks the Conseil Régional de Bourgogne, the Ministère de l'Enseignement Supérieur et de la Recherche, and the Centre National de la Recherche Scientifique (CNRS) for financial support. We thank the Partenariat Hubert Curien (PHC) Franco-Suisse "Germaine de Staël" (project no. 2010-01/21760SJ, "Novel bimetallic complexes as highly efficient anticancer agents").

References

(1) Rosenberg, B.; VanCamp, L.; Trosko, J. E.; Mansour, V. H. Platinum compounds: a new class of potent antitumor agents. *Nature* **1969**, *222*, 385–386.
(2) Muggia, F. Platinum compounds 30 years after the introduction of cisplatin: implications for the treatment of ovarian cancer. *Gynecol. Oncol.* **2009**, *112*, 275–281.

(3) Rabik, C. A.; Dolan, M. E. Molecular mechanisms of resistance and toxicity associated with platinating agents. *Cancer Treat. Rev.* **2007**, *33*, 9–23.
(4) Farrell, N. Current status of structure−activity relationships of platinum anticancer drugs: activation of the trans geometry. *Met. Ions Biol. Syst.* **1996**, *32*, 603–639.
(5) (a) Vessières, A.; Top, S.; Beck, W.; Hillard, E.; Jaouen, G. Metal complex SERMs (selective oestrogen receptor modulators). The influence of different metal units on breast cancer cell antiproliferative effects. *Dalton Trans.* **2006**, *28*, 529–541. (b) Hartinger, C. G.; Dyson, P. J. Bioorganometallic chemistry—from teaching paradigms to medicinal applications. *Chem. Soc. Rev.* **2009**, *38*, 391–401. (c) Nobili, S.; Mini, E.; Landini, I.; Gabbiani, C.; Casini, A.; Messori, L. Gold compounds as anticancer agents: chemistry, cellular pharmacology, and preclinical studies. *Med. Res. Rev.* **2010**, *30*, 550–580.
(6) (a) Müller, B. W.; Lucks, S.; Müller, R.; Mohr, W. Wasserlösliche pharmazeutische metallocen−komplex−zusammensetzung. Eur. Patent 0,407,804, 1991. (b) Müller, B. W.; Müller, R.; Lucks, S.; Mohr, W. Water−soluble pharmaceutical metallocene−complex composition. U.S. Patent 5,296,237, 1994.
(7) Hartinger, C. G.; Zorbas-Seifried, S.; Jakupec, M. A.; Kynast, B.; Zorbas, H.; Keppler, B. K. From bench to bedside—preclinical and early clinical development of the anticancer agent indazolium *trans*-[tetrachlorobis(1*H*-indazole)ruthenate(III)] (KP1019 or FFC14A). *J. Inorg. Biochem.* **2006**, *100*, 891–904.
(8) Rademaker-Lakhai, J. M.; van der Bongard, D.; Pluim, D.; Beijnen, J. H.; Schellens, J. H. M. A phase I and pharmacological study with imidazolium-*trans*-DMSO-imidazole-tetrachlororuthenate, a novel ruthenium anticancer agent. *Clin. Cancer. Res.* **2004**, *10*, 3717–3727.
(9) (a) Morris, R. E.; Aird, R. E.; Murdoch, P. d. S.; Chen, H.; Cummings, J.; Hughes, N. D.; Parsons, S.; Parkin, A.; Boyd, G.; Jodrell, D. I.; Sadler, P. J. Inhibition of cancer cell growth by ruthenium(II) arene complexes. *J. Med. Chem.* **2001**, *44*, 3616–3621. (b) Akbayeva, D. N.; Gonsalvi, L.; Oberhauser, W.; Peruzzini, M.; Vizza, F.; Brüggeller, P.; Romerosa, A.; Sava, G.; Bergamo, A. Synthesis, catalytic properties and biological activity of new water soluble ruthenium cyclopentadienyl PTA complexes $[(C_5R_5)RuCl(PTA)_2]$ (R = H, Me; PTA = 1,3,5-triaza-7-phosphaadamantane). *Chem. Commun.* **2003**, 264–265. (c) Vock, C. A.; Scolaro, C.; Phillips, A. D.; Scopelliti, R.; Sava, G.; Dyson, P. J. Synthesis, characterization, and in vitro evaluation of novel ruthenium(II) η^6-arene imidazole complexes. *J. Med. Chem.* **2006**, *49*, 5552–5561. (d) Romerosa, A.; Campos-Malpartida, T.; Lidrissi, C.; Saoud, M.; Serrano-Ruiz, M.; Peruzzini, M.; Garrido-Cárdenas, J. A.; García-Maroto, F. Synthesis, characterization and DNA binding of new water-soluble cyclopentadienyl ruthenium(II) complexes incorporating phosphines. *Inorg. Chem.* **2006**, *45*, 1289–1298. (e) Schmid, W. F.; John, O. R.; Mühlgassner, G.; Heffeter, P.; Jakupec, M. A.; Galanski, M.; Berger, W.; Arion, V. B.; Keppler, B. K. Metal-based paullones as putative CDK inhibitors for antitumor chemotherapy. *J. Med. Chem.* **2007**, *50*, 6343–6355. (f) Schmid, W. F.; John, O. R.; Arion, V. B.; Jakupec, M. A.; Keppler, B. K. Highly antiproliferative ruthenium(II) and osmium(II) arene complexes with paullone-derived ligands. *Organometallics* **2007**, *26*, 6643–6652. (g) Vock, C. A.; Ang, W. H.; Scolaro, C.; Phillips, A. D.; Lagopoulos, L.; Juillerat-Jeanneret, L.; Sava, G.; Scopelliti, R.; Dyson, P. J. Development of ruthenium antitumor drugs that overcome multidrug resistance mechanisms. *J. Med. Chem.* **2007**, *50*, 2166–2175. (h) Ang, W. H.; De Luca, A.; Chapuis-Bernasconi, C.; Juillerat-Jeanneret, L.; Lo Bello, M.; Dyson, P. J. Organometallic ruthenium inhibitors of glutathione-S-transferase P1−1 as anticancer drugs. *ChemMedChem* **2007**, *2*, 1799–1806. (i) Peacock, A. F. A.; Sadler, P. J. Medicinal organometallic chemistry: designing metal arene complexes as anticancer agents. *Chem. Asian J.* **2008**, *3*, 1890–1899. (j) Govender, P.; Antonels, N. C.; Mattsson, J.; Renfrew, A. K.; Dyson, P. J.; Moss, J. R.; Therrien, B.; Smith, G. S. Anticancer activity of multinuclear arene ruthenium complexes coordinated to dendritic polypyridyl scaffolds. *J. Organomet. Chem.* **2009**, *694*, 3470–3476. (k) Rajapakse, C. S. K.; Martínez, A.; Naoulou, B.; Jarzecki, A. A.; Suárez, L.; Deregnaucourt, C.; Sinou, V.; Schrével, J.; Musi, E.; Ambrosini, G.; Schwartz, G. K.; Sánchez-Delgado, R. A. Synthesis, characterization, and in vitro antimalarial and antitumor activity of new ruthenium(II) complexes of chloroquine. *Inorg. Chem.* **2009**, *48*, 1122–1131. (l) Kandioller, W.; Hartinger, C. G.; Nazarov, A. A.; Kasser, J.; Roland, J.; Jakupec, M. A.; Arion, V. B.; Dyson, P. J.; Keppler, B. K. Tuning the anticancer activity of maltol-derived ruthenium complexes by derivatization of the 3-hydroxy-4-pyrone moiety. *J. Organomet. Chem.* **2009**, *694*, 922–929. (m) Mendoza-Ferri, M. G.; Hartinger, C. G.; Nazarov, A. A.; Eichinger, R. E.; Jakupec, M. A.; Severin, K.; Keppler, B. K. Influence of the arene ligand, the number and type of metal centers, and the leaving group on the in vitro antitumor activity of polynuclear organometallic compounds. *Organometallics* **2009**, *28*, 6260–6265. (n) Levina, A.; Mitra, A.; Lay, P. A. Recent developments in ruthenium anticancer drugs. *Metallomics* **2009**, *1*, 458–470. (o) Kandioller, W.; Hartinger, C. G.; Nazarov, A. A.; Kuznetsov, M. L.; John, R. O.; Bartel, C.; Jakupec, M. A.; Arion, V. B.; Keppler, B. K. From pyrone to thiopyrone ligands-rendering maltol-derived ruthenium(II)-arene complexes that are anticancer active in vitro. *Organometallics* **2009**, *28*, 4249–4251.
(10) (a) Scolaro, C.; Bergamo, A.; Brescacin, L.; Delfino, R.; Cocchietto, M.; Laurenczy, G.; Geldbach, T. J.; Sava, G.; Dyson, P. J. In vitro and in vivo evaluation of ruthenium(II)-arene PTA complexes. *J. Med. Chem.* **2005**, *48*, 4161–4171. (b) Bergamo, A.; Masi, A.; Dyson, P. J.; Sava, G. Modulation of the metastatic progression of breast cancer with an organometallic ruthenium compound. *Int. J. Oncol.* **2008**, *33*, 1281–1289. (c) Chatterjee, S.; Kundu, S.; Bhattacharyya, A.; Hertinger, C. G.; Dyson, P. J. The ruthenium(II)-arene compound RAPTA-C induces apoptosis in EAC cells through mitochondrial and p53−JNK pathways. *J. Biol. Inorg. Chem.* **2008**, *13*, 1149–1155.
(11) (a) Allardyce, C. S.; Dyson, P. J.; Ellis, D. J.; Heath, S. L. [Ru(η^6-*p*-cymene)Cl_2(pta)] (pta = 1,3,5-triaza-7-phosphatricyclo-[3.3.1.1]-decane): a water soluble compound that exhibits pH dependent DNA binding providing selectivity for diseased cells. *Chem. Commun.* **2001**, 1396–1397. (b) Ang, W. H.; Daldini, E.; Scolaro, C.; Scopelliti, R.; Juillerat-Jeannerat, L.; Dyson, P. J. Development of organometallic ruthenium-arene anticancer drugs that resist hydrolysis. *Inorg. Chem.* **2006**, *45*, 9006–9013. (c) Scolaro, C.; Geldbach, T. J.; Rochat, S.; Dorcier, A.; Gossens, C.; Bergamo, A.; Cocchietto, M.; Tavernelli, I.; Sava, G.; Rothlisberger, U.; Dyson, P. J. Influence of hydrogen-bonding substituents on the cytotoxicity of RAPTA compounds. *Organometallics* **2006**, *25*, 756–765. (d) Ang, W. H.; Daldini, E.; Juillerat-Jeanneret, L.; Dyson, P. J. Strategy to tether organometallic ruthenium-arene anticancer compounds to recombinant human serum albumin. *Inorg. Chem.* **2007**, *46*, 9048–9050. (e) Vock, C. A.; Renfrew, A. K.; Scopelliti, R.; Juillerat-Jeanneret, L.; Dyson, P. J. Influence of the diketonato ligand on the cytotoxicities of [Ru(η^6-p-cymene)-(R_2acac)-(PTA)]$^+$ complexes (PTA = 1,3,5-triaza-7-phosphaadamantane). *Eur. J. Inorg. Chem.* **2008**, 1661–1671. (f) Renfrew, A. K.; Phillips, A. D.; Tapaviscza, E.; Scopelliti, R.; Rothlisberger, U.; Dyson, P. J. Tuning the efficacy of ruthenium(II)-arene (RAPTA) antitumor compounds with fluorinated arene ligands. *Organometallics* **2009**, *28*, 5061–5071. (g) Renfrew, A. K.; Phillips, A. D.; Egger, A. E.; Hartinger, C. G.; Bosquain, S. S.; Nazarov, A. A.; Keppler, B. K.; Gonsalvi, L.; Peruzzini, M.; Dyson, P. J. Influence of structural variation on the anticancer activity of RAPTA-type complexes: ptn versus pta. *Organometallics* **2009**, *28*, 1165–1172.
(12) (a) Top, S.; Kaloun, E. B.; Vessières, A.; Laïos, I.; Leclercq, G.; Jaouen, G. The first titanocenyl dichloride moiety vectorised by a selective estrogen receptor modulator (SERM). Synthesis and preliminary biochemical behaviour. *J. Organomet. Chem.* **2002**, *643−644*, 350–356. (b) Allen, O. R.; Croll, L.; Gott, A. L.; Knox, R. J.; McGowan, P. C. Functionalized cyclopentadienyl titanium organometallic compounds as new antitumor drugs. *Organometallics* **2004**, *23*, 288–292. (c) Causey, P. W.; Baird, M. C.; Cole, S. P. C. Synthesis, characterization, and assessment of cytotoxic properties of a series of titanocene dichloride derivatives. *Organometallics* **2004**, *23*, 4486–4494. (d) Tacke, M.; Allen, L. T.; Cuffe, L.; Gallagher, W. L.; Lou, Y.; Mendoza, O.; Müller-Bunz, H.; Rehmann, F.-J. K.; Sweeney, N. Novel titanocene anti-cancer drugs derived from fulvenes and titanium dichloride. *J. Organomet. Chem.* **2004**, *689*, 2242–2249. (e) Potter, G. D.; Baird, M. C.; Cole, S. P. C. A new series of titanocene dichloride derivatives bearing cyclic alkylammonium groups: assessment of their cytotoxic properties. *J. Organomet. Chem.* **2007**, *692*, 3508–3518. (f) Pampillón, C.; Claffey, J.; Hogan, M.; Tacke, M. Novel achiral titanocene anti-cancer drugs synthesised from bis-N,N-dimethylamino fulvene and lithiated heterocyclic compounds. *Biometals* **2008**, *21*, 197–204. (g) Hogan, M.; Cotter, J.; Claffey, J.; Gleeson, B.; Wallis, D.; O'Shea, D.; Tacke, M. Synthesis and cytotoxicity studies of new (dimethylamino)-functionalised and 7-azaindole-substituted-titanocene anticancer agents (7-azaindole-1H-pyrrolo[2,3-b]pyridine). *Helv. Chim. Acta* **2008**, *91*, 1787–1797. (h) Pampillón, C.; Claffey, J.; Strohfeldt, K.; Tacke, M. Synthesis and cytotoxicity studies of new dimethylamino-functionalised and aryl-substituted titanocene anti-cancer agents. *Eur. J. Med. Chem.* **2008**, *43*, 122–128.
(13) (a) Sweeney, N. J.; Mendoza, O.; Müller-Bunz, H.; Pampillón, C.; Rehmann, F.-J. K.; Strohfeldt, K.; Tacke, M. Novel benzyl substituted titanocene anti-cancer drugs. *J. Organomet. Chem.* **2005**, *690*, 4537–4544. (b) Pampillón, C.; Mendoza, O.; Sweeney, N. J.; Strohfeldt, K.; Tacke, M. Diarylmethyl substituted titanocenes: promising anti-cancer drugs. *Polyhedron* **2006**, *25*, 2101–2108. (c) Strohfeldt, K.; Müller-Bunz, H.; Pampillón, C.; Sweeney, N. J.; Tacke, M. Glycol methyl ether and glycol amine substituted titanocenes as antitumor agents. *Eur. J. Inorg. Chem.* **2006**, 4621–4628. (d) Claffey, J.; Hogan, M.;

Müller-Bunz, H.; Pampillón, C.; Tacke, M. Synthesis and cytotoxicity studies of methoxy benzyl substituted titanocenes. *J. Organomet. Chem.* **2008**, *693*, 526–536. (e) Vessières, A.; Plamont, M.-A.; Cabestaing, C.; Claffey, J.; Dieckmann, S.; Hogan, M.; Müller-Bunz, H.; Strohfeldt, K.; Tacke, M. Proliferative and anti-proliferative effects of titanium- and iron-based metallocene anti-cancer drugs. *J. Organomet. Chem.* **2009**, *694*, 874–879.

(14) Tshuva, E. Y.; Ashenhurst, J. A. Cytotoxic Titanium(IV) Complexes: Renaissance. *Eur. J. Inorg. Chem.* **2009**, 2203–2218.

(15) Bannon, J. H.; Fichtner, I.; O'Neill, A.; Pampillón, C.; Sweeney, N. J.; Strohfeldt, K.; Watson, R. W.; Tacke, M.; Mc Gee, M. M. Substituted titanocenes induce caspase-dependent apoptosis in human epidermoid carcinoma cells in vitro and exhibit antitumour activity in vivo. *Br. J. Cancer* **2007**, *97*, 1234–1241.

(16) An attempt to draw a general scheme for the mechanism of action of ruthenium metallodrugs was recently published, see ref 9n.

(17) (a) Dyson, P. J.; Sava, G. Metal-based antitumour drugs in the post genomic era. *Dalton Trans.* **2006**, 1929–1933. (b) Ang, W. H.; Parker, L. J.; De luca, A.; Juillerat-Jeanneret, L.; Morton, C. J.; Lo Bello, M.; Parker, M. W.; Dyson, P. J. Rational design of an organometallic glutathione transferase inhibitor. *Angew. Chem., Int. Ed.* **2009**, *48*, 3854–3857. (c) Casini, A.; Karotki, A.; Gabbiani, C.; Rugi, F.; Vasak, M.; Messori, L.; Dyson, P. J. Reactivity of an antimetastatic organometallic ruthenium compound with metallothionein-2: relevance to the mechanism of action. *Metallomics* **2009**, *1*, 434–441.

(18) (a) Casini, A.; Gabbiani, C.; Sorrentino, F.; Rigobello, M. P.; Bindoli, A.; Geldbach, T. J.; Marrone, A.; Re, N.; Hartinger, C. G.; Dyson, P. J.; Messori, L. Emerging protein targets for anticancer metallodrugs: inhibition of thioredoxin reductase and cathepsin B by antitumor ruthenium(II)-arene compounds. *J. Med. Chem.* **2008**, *51*, 6773–6781. (b) Mura, P.; Camalli, M.; Casini, A.; Gabbiani, C.; Messori, L. trans-cis-cis-[$RuCl_2(DMSO)_2$(2-amino-5-methylthiazole)$_2$], (PMRu52), a novel ruthenium(II) compound acting as a strong inhibitor of cathepsin B. *J. Inorg. Biochem.* **2010**, *104*, 111–117.

(19) (a) Koblinski, J. E.; Ahram, M.; Sloane, B. F. Unraveling the role of proteases in cancer. *Clin. Chim. Acta* **2000**, *291*, 113–135. (b) Mohanam, S.; Jasti, S. L.; Kondraganti, S. R.; Chandrasekar, N.; Lakka, S. S.; Kin, Y.; Fuller, G. N.; Yung, A. W. K.; Kyritsis, A. P.; Dinh, D. H.; Olivero, W. C.; Gujrati, M.; Ali-Osman, F.; Rao, J. S. Down-regulation of cathepsin B expression impairs the invasive and tumorigenic potential of human glioblastoma cells. *Oncogene* **2001**, *20*, 3665–3673.

(20) Bergamo, A.; Masi, A.; Dyson, P. J.; Sava, G. Modulation of the metastatic progression of breast cancer with an organometallic ruthenium compound. *Int. J. Oncol.* **2008**, *33*, 1281–1289.

(21) (a) Murray, J. H.; Harding, M. M. Organometallic anticancer agents: the effect of the central metal and halide ligands on the interaction of metallocenes dihalides Cp_2MX_2 with nucleic acid constituents. *J. Med. Chem.* **1994**, *37*, 1936–1941. (b) Kostova, I. Titanium and vanadium complexes as anticancer agents. *Anti-Cancer Agents Med. Chem.* **2009**, *9*, 827–842.

(22) (a) Guo, M.; Sun, H.; McArdle, H. J.; Gambling, L.; Sadler, P. J. Ti^{IV} uptake and release by human serum transferrin and recognition of Ti^{IV}-transferrin by cancer cells: understanding the mechanism of action of the anticancer drug titanocene dichloride. *Biochemistry* **2000**, *39*, 10023–10033. (b) Guo, M.; Guo, Z.; Sadler, P. J. Titanium(IV) targets phosphoesters on nucleotides: implications for the mechanism of action of the anticancer drug titanocene dichloride. *J. Biol. Inorg. Chem.* **2001**, *6*, 698–707. (c) Olszewski, U.; Claffey, J.; Hogan, M.; Tacke, M.; Zeillinger, R.; Bednarski, P. J.; Hamilton, G. Anticancer activity and mode of action of titanocene C. *Invest. New Drugs* **2010**, DOI: 10.1007/s10637-010-9395-5.

(23) (a) Therrien, B.; Ang, W. H.; Chérioux, F.; Vieille-Petit, L.; Juillerat-Jeanneret, L.; Süss-Fink, G.; Dyson, P. J. Remarkable anticancer activity of triruthenium-arene clusters compared to tetraruthenium-arene clusters. *J. Cluster Sci.* **2007**, *18*, 741–752. (b) Mendoza-Ferri, M. G.; Hartinger, C. G.; Eichinger, R. E.; Stolyarova, N.; Severin, K.; Jakupec, M. A.; Nazarov, A. A.; Keppler, B. K. Influence of the spacer length on the in vitro anticancer activity of dinuclear ruthenium-arene compounds. *Organometallics* **2008**, *27*, 2405–2407. (c) Mendoza-Ferri, M. G.; Hartinger, C. G.; Nazarov, A. A.; Kandioller, W.; Severin, K.; Keppler, B. K. Modifying the structure of dinuclear ruthenium complexes with antitumor activity. *Appl. Organomet. Chem.* **2008**, *22*, 326–332. (d) Schmitt, F.; Govindaswamy, P.; Süss-Fink, G.; Ang, W. H.; Dyson, P. J.; Juillerat-Jeanneret, L.; Therrien, B. Ruthenium Porphyrin Compounds for Photodynamic Therapy of Cancer. *J. Med. Chem.* **2008**, *51*, 1811–1816. (e) Gabbiani, C.; Casini, A.; Messori, L.; Guerri, A.; Cinellu, M. A.; Minghetti, G.; Corsini, M.; Rosani, C.; Zanello, P.; Arca, M. Structural characterization, solution studies, and DFT calculations on a series of binuclear gold(III) oxo complexes: relationships to biological properties. *Inorg. Chem.* **2008**, *47*, 2368–2379. (f) Kong, K. V.; Leong, W. K.; Lim, L. H. K. Induction of apoptosis by hexaosmium carbonyl clusters. *J. Organomet. Chem.* **2009**, *694*, 834–839. (g) Ang, W. H.; Grote, Z.; Scopelliti, R.; Juillerat-Jeanneret, L.; Severin, K.; Dyson, P. J. Organometallic complexes that interconvert between trimeric and monomeric structures as a function of pH and their effect on human cancer and fibroblast cells. *J. Organomet. Chem.* **2009**, *694*, 968–972. (h) Mattsson, J.; Govindaswamy, P.; Renfrew, A. K.; Dyson, P. J.; Stepnicka, P.; Süss-Fink, G.; Therrien, B. Synthesis, molecular structure, and anticancer activity of cationic arene ruthenium metallarectangles. *Organometallics* **2009**, *28*, 4350–4357. (i) Ott, I. On the medicinal chemistry of gold complexes as anticancer drugs. *Coord. Chem. Rev.* **2009**, *253*, 1670–1681.

(24) (a) Henderson, W.; Alley, S. Platinum(II) complexes containing ferrocene-derived phosphonate ligands; synthesis, structural characterisation and antitumour activity. *Inorg. Chim. Acta* **2001**, *322*, 106–112. (b) Tiekink, E. R. T. Gold derivatives for the treatment of cancer. *Crit. Rev. Oncol./Hematol.* **2002**, *42*, 225–248. (c) Wedgwood, J. L.; Kresinski, R. A.; Merry, S.; Platt, A. W. G. The preparation, characterisation and in vitro cytotoxicity of potentially chemotherapeutic heterobimetallic complexes containing early and late transition metals. *J. Inorg. Biochem.* **2003**, *95*, 149–156. (d) van der Schilden, K.; Garca, F.; Kooijman, H.; Spek, A. L.; Haasnoot, J. G.; Reedijk, J. A Highly flexible dinuclear ruthenium(II)−platinum(II) complex: crystal structure and binding to 9-ethylguanine. *Angew. Chem., Int. Ed.* **2004**, *43*, 5668–5670. (e) de Hoog, P.; Boldron, C.; Gamez, P.; Sliedregt-Bol, K.; Roland, I.; Pitie, M.; Kiss, R.; Meunier, B.; Reedijk, J. New approach for the preparation of efficient DNA cleaving agents: ditopic copper−platinum complexes based on 3-clip-phen and cisplatin. *J. Med. Chem.* **2007**, *50*, 3148–3152. (f) Auzias, M.; Therrien, B.; Süss-Fink, G.; Stepnicka, P.; Ang, W. H.; Dyson, P. J. Ferrocenoyl pyridine arene ruthenium complexes with anticancer properties: Synthesis, structure, electrochemistry, and cytotoxicity. *Inorg. Chem.* **2008**, *47*, 578–583. (g) Therrien, B.; Süss-Fink, G.; Govindaswamy, P.; Renfrew, A. K.; Dyson, P. J. The "complex-in-a-complex" cations $[(acac)_2M\subset Ru_6$-(p-iPrC_6H_4Me)$_6$(tpt)$_2$(dhbq)$_3]^{6+}$: a Trojan horse for cancer cells. *Angew. Chem., Int. Ed.* **2008**, *47*, 3773–3776. (h) Auzias, M.; Gueniat, J.; Therrien, B.; Süss-Fink, G.; Renfrew, A. K.; Dyson, P. J. Arene−ruthenium complexes with ferrocene-derived ligands: synthesis and characterization of complexes of the type [Ru(η^6-arene)-($NC_5H_4CH_2NHOC$-$C_5H_4FeC_5H_5$)Cl_2] and [Ru(η^6-arene)(NC_3H_3N-$(CH_2)_2O_2C$−$C_5H_4FeC_5H_5$)Cl_2]. *J. Organomet. Chem.* **2009**, *694*, 855–861.

(25) (a) Le Gendre, P.; Richard, P.; Moïse, C. Synthesis and structural studies of Ti−Ru polymetallic systems. *J. Organomet. Chem.* **2000**, *605*, 151–156. (b) Bareille, L.; Le Gendre, P.; Richard, P.; Moïse, C. Towards a library of "early−late" Ti−Ru bimetallic complexes. *Eur. J. Inorg. Chem.* **2005**, 2451–2456. (c) Le Gendre, P.; Picquet, M.; Richard, P.; Moïse, C. Ti−Ru bimetallic complexes: catalysts for ring-closing metathesis. *J. Organomet. Chem.* **2002**, *643−644*, 231–236.

(26) Bredeau, S.; Altenhoff, G.; Kunz, K.; Döring, S.; Grimme, S.; Kehr, G.; Erker, G. Synthesis of alkylidene-bridged Cp/phosphido group 4 metal complexes−precursors of the "(CpCPR)M−constrained-geometry" catalyst family. *Organometallics* **2004**, *23*, 1836–1844.

(27) Todd, R. C.; Lippard, S. J. Inhibition of transcription by platinum antitumor compounds. *Metallomics* **2009**, *1*, 280–291.

(28) Fricker, S. P. Cysteine proteases as targets for metal-based drugs. *Metallomics* **2010**, *2*, 366–377.

(29) Christodoulou, C. V.; Eliopoulos, A. G.; Young, L. S.; Hodgkins, L.; Ferry, D. R.; Kerr, D. J. Anti-proliferative activity and mechanism of action of titanocene dichloride. *Br. J. Cancer* **1998**, *77*, 2088–2097.

(30) Musil, D.; Zucic, D.; Turk, D.; Engh, R. A.; Mayr, I.; Huber, R.; Popovic, T.; Turk, V.; Towatari, T.; Katunuma, N.; Bode, W. The refined 2.15 Å X-ray crystal structure of human liver cathepsin B: the structural basis for its specificity. *EMBO J.* **1991**, *10*, 2321–2330.

(31) (a) Peleg-Shulman, T.; Najajreh, Y.; Gibson, D. Interactions of cisplatin and transplatin with proteins. Comparison of binding kinetics, binding sites and reactivity of the Pt−protein adducts of cisplatin and transplatin towards biological nucleophiles. *J. Inorg. Biochem.* **2002**, *91*, 306–311. (b) Hartinger, C. G.; Wee, H. A.; Casini, A.; Messori, L.; Keppler, B. K.; Dyson, P. J. Mass spectrometric analysis of ubiquitin−platinum interactions of leading anticancer drugs: MALDI versus ESI. *J. Anal. At. Spectrom.* **2007**, *22*, 960–967. (c) Casini, A.; Guerri, A.; Gabbiani, C.; Messori, L. Biophysical characterisation of adducts formed between anticancer metallodrugs and selected proteins: new insights from X-ray diffraction and mass spectrometry studies. *J. Inorg. Biochem.* **2008**, *102*, 995–1006. (d) Hartinger, C. G.; Casini, A.; Duhot, C.; Tsybin, Y. O.; Messori, L.; Dyson, P. J. Stability of an organometallic ruthenium−ubiquitin

adduct in the presence of glutathione: relevance to antitumour activity. *J. Inorg. Biochem.* **2008**, *102*, 2136–2141.
(32) (a) Jaouen, G.; Top, S.; Vessières, A.; Leclercq, G.; McGlinchey, M. J. The first organometallic selective estrogen receptor modulators (SERMs) and their relevance to breast cancer. *Curr. Med. Chem.* **2004**, *11*, 2505–2517. (b) Kirin, S. I.; Kraatz, H. B.; Metzler-Nolte, N. Systematizing structural motifs and nomenclature in 1,n′-disubstituted ferrocene peptides. *Chem. Soc. Rev.* **2006**, *35*, 348–354. (c) Dyson, P. J. Systematic design of a targeted organometallic antitumour drug in pre-clinical development. *Chimia* **2007**, *61*, 698–703.
(33) Spencer, J.; Casini, A.; Zava, O.; Rathnam, R. P.; Velhanda, S. K.; Pfeffer, M.; Callear, S. K.; Hursthouse, M. B.; Dyson, P. J. Excellent correlation between cathepsin B inhibition and cytotoxicity for a series of palladacycle. *Dalton Trans.* **2009**, 10731–10735.
(34) Leblanc, J.-C.; Moïse, C.; Maisonnat, A.; Poilblanc, R.; Charrier, C.; Mathey, F. Complexes du titane et du zirconium contenant les ligands cyclopentadiényldiphénylphosphine et cyclopentadiényléthyldiphénylphosphine: accès à des structures hétérobimétalliques *J. Organomet. Chem.* **1982**, *231*, C43–C48.
(35) Baraut, J.; Perrier, A.; Comte, V.; Picquet, M.; Moïse, C.; Le Gendre, P. Unpublished results .
(36) Altomare, A.; Cascarano, G.; Giacovazzo, C.; Guagliardi, A. Completion and refinement of crystal structures with SIR92. *J. Appl. Crystallogr.* **1993**, *26*, 343–350.
(37) Sheldrick, G. M., *SHELX97* (*Includes SHELXS97 and SHELXL97*), *Release 97-2, Programs for Crystal Structure Analysis*; Institüt für Anorganische Chemie, University of Göttingen, Tammanstrasse 4, D-3400 Göttingen, Germany, 1998.
(38) Farrugia, L. J. WinGX suite for small molecule single-crystal crystallography. *J. Appl. Crystallogr.* **1999**, *32*, 837–838.